Early evolution of a young back-arc basin in the Havre Trough

Fabio Caratori Tontini[1], Dan Bassett[1], Cornel E. J. de Ronde[1], Christian Timm[1,2] and Richard Wysoczanski[3]

[1]GNS Science, Lower Hutt, New Zealand

[2]GEOMAR, Helmholtz Centre for Ocean Research, Kiel, Germany

[3]NIWA, Wellington, New Zealand

FIRST PARAGRAPH

Back-arc basins are found at convergent plate boundaries. Nevertheless, they are zones of significant crustal extension, showing volcanic and hydrothermal processes somewhat similar to mid-ocean ridges. Accepted models imply initial rifting and thinning of a pre-existing volcanic arc until seafloor spreading gradually develops over time-scales of few Myr. The Havre Trough northeast of New Zealand is a unique place on Earth where the early stages of back-arc basin formation are well displayed in the recent geological record. Here we present evidence that in this region, rifting of the original volcanic arc occurred in a very narrow area about 10-15 km wide, which could only accommodate minimal stretching for a very short time before mass balance would require oceanic crustal accretion. An initial burst of seafloor spreading started around 5.5-5.0 Ma and concluded abruptly about 3.0-2.5 Ma, after which arc magmatism dominated crustal accretion. The sudden transition between these different tectono-magmatic regimes is linked to trench rollback promoted by gradual sinking of the subducting lithosphere, which could have diverted the arc flux outside of the region of seafloor spreading inducing the vertical realignment of surface volcanism with the source of arc melts at depth.

The opening of back-arc basins starts with initial rifting and crustal thinning of a pre-existing volcanic arc[1-3] until a critical amount of stretching is reached, after which further extension is accommodated by the formation of new oceanic crust[4-8]. The Havre Trough is a submarine extensional basin bordered by the Colville Ridge remnant arc to the west and the Kermadec Ridge to the east (Figure 1), related to the subduction of the Pacific Plate and the Hikurangi Plateau underneath the Australian Plate[12-15]. The northern extension of the Havre Trough is the Lau Basin[4,7,8], whereas its southern continuation is the active continental rift known as the Taupo Volcanic Zone (TVZ)[16-19].

Initial splitting of the original proto-Colville-Kermadec arc is thought to have started ~5.5 Ma[13,16,18,20-22] in response to the rollback of the subducting Pacific Plate[23,24]. Oblique extension progressively propagated south[18,21,22] from the Lau Basin, with an estimated extension rate of ~15-25 mm/yr[16,18,20] in the Havre Trough consistent with present-day velocities from geodetic retriangulation onshore North Island[25,26], seismological slip vector data offshore[22,27,28] and GPS data[29].

High heat-flow[1,16,19], shallow seismicity[15,16], lavas with a more pronounced Island Arc Basalt (IAB) signature moving eastward towards the Kermadec arc front[20,21,30] and crustal seismic velocities similar to normal oceanic crust[1,11,14] suggest that the Havre Trough could be actively spreading. However, the controversial interpretation of low-resolution magnetic anomalies[13,31] and the absence of an obvious spreading ridge[16], do not support present-day seafloor spreading but rather imply that the Havre Trough is still in a phase of rifting[16,18,32].

Observations from bathymetric and geophysical surveys

Bathymetric, gravity and magnetic surveys (Figure 2) reveal a sharp contrast in the structure of the Eastern and Western segments of the Havre Trough. The bathymetry (Figure 2a) shows that the seafloor morphology in the Western Havre Trough is dominated by a set of segmented and discrete en echelon extensional basins up to 4000 m deep. The morphology of these basins does not show a clear spreading ridge like those found in the Lau Basin or Mariana Trough[4-8] but is rather characterized by flat floors and thicker sediment infills, up to 400-800 m[11,13,21], indicating lack of recent neovolcanic activity in these areas. These basins are interrupted along strike by younger cross-arc massifs and seamounts characterized by IAB composition, possibly recording the migration from the proto-Colville-Kermadec arc to the present active volcanic front[20], or younger volcanism along pre-existing cross-arc structures[34,35].

In contrast, the morphology of the Eastern Havre Trough is characterized by shallower bathymetry and appears dominated by the construction of young volcanic edifices which constitute the active Kermadec arc front and smaller extensional basins. These basins are narrower, shallower and practically unsedimented[11]. This contrast in basin morphology and sediment thickness indicate current active extensional deformation in the Eastern Havre Trough, and a cessation of deformation in the Western Havre Trough. The clear boundary between Western and Eastern Havre Trough, along the easternmost black dashed-line in Figure 2, indicates a sharp discontinuity along a median line approximately equidistant from the Colville and Kermadec Ridges.

This contrast is also clearly expressed by the magnetic anomaly map in Figure 2b. The Western Havre Trough is characterized by long magnetic lineations with alternating polarities which run parallel to the Colville Ridge and strike for ~ 500 km. There is a change in the pattern of these magnetic lineations between 34° S and 35° S, where the central normal polarity is gradually replaced by a central reversed polarity towards the south. We can delineate three different zones (I, II, and III in Figure 2) based on this magnetic transition with boundaries which are defined by cross-arc constructional features in the bathymetry map of Figure 2a. The eastern Havre Trough, by contrast, does not show a systematic pattern of magnetic lineations but rather a system of localized magnetic anomalies strongly correlated with bathymetry variations. The boundary between Western and Eastern Havre Trough is also visible in the free-air gravity map of Figure 2c. West of this boundary the gravity data are characterized by local lows over a baseline of ~50 mGal, whereas east of this boundary, gravity is dominated by highs > 100 mGal. The Bouguer gravity map in Figure 2d, where the effect of seafloor bathymetry is removed, shows a widespread gravity high in the Havre Trough.

The clearest evidence of the sharp boundary and the differences between Western and Eastern Havre Trough is shown in the seismic sections in Figure 3. P-wave velocities from seismic refraction data (Figure 3a) show an abrupt discontinuity in the centre of the Havre Trough. The Western Havre Trough is characterized by a thick layer of sediments (Figure 3b), whereas the Eastern Havre Trough is lacking any visible sediment cover. The seafloor fabric also shows rough bathymetry characterized by alternating reliefs and depressions in the Eastern Havre Trough, in contrast with almost flat seafloor in the Western Havre Trough. P-wave velocity and seismic reflection data show evidence of a buried ridge under the sediments, with a local thinning of the overlying sediments from 400-800 m to of ~ 180 m (estimated using a V_p of 1.8 $km \cdot s^{-1}$) at the center of the Western Havre Trough (~ Distance 82 km in Figure 3a and CPD 570 in Figure 3b).

Evidence of past seafloor spreading in the Havre Trough

There is a clear geophysical evidence of *past* seafloor spreading in the Western Havre Trough. This region represents the initial phase of extension after breakup of the original proto-Colville-Kermadec arc and does not show evidence of present-day extensional deformation. The thick layer of sediments may have blanketed evidence of a spreading ridge in the bathymetry, however the seismic sections in Figure 3 show a buried ridge at the center of the Western Havre Trough. Similar evidence is observed elsewhere along the back-arc[11,13] and could represent the seismic expression of a buried spreading ridge.

The estimated average rate of sedimentation from very few sites[36,37] in this region for the last 50 ka is ~70 mm/kyr. Extrapolation of this rate would suggest that the ~180 m of sedimentary succession overlying the buried ridge at the center of the Western Havre Trough accumulated in the last ~2.6 Myr. However, this is a not a robust estimate because sedimentation in this volcanic environment is not continuous and is affected by episodic volcanic eruption which could provide irregular rates. Alternatively, if rifting of the original proto-Colville-Kermadec arc started ~5.5 Ma and continued at a constant opening rate of ~20 mm/yr, we predict a width for the Havre Trough of ~110 km, which is consistent with the observed width of ~100-120 km (Figure 2a). In this case, because the Western Havre Trough has an average width of ~50-60 km, it must have formed during the first 2.5-3.0 Myr of extension and abruptly terminated ~3.0-2.5 Ma, still compatible with the previous estimate of ~ 2.6 Ma from sediment thickness.

The last 6 Myr are characterized by four magnetic epochs[38] with alternating polarities, supporting the hypothesis of seafloor spreading in the Western Havre Trough. In the central and northern sector (zone I and zone II), the central lineation has normal polarity and is flanked either side by adjacent lineations with reversed polarities. The older lineations indicate initiation of spreading during the Gilbert epoch[38] (5.89-3.58 Ma), i.e., almost synchronous with the initial splitting of the proto-Colville-Kermadec arc. The average total width of these anomalies of ~ 35-40 km (Figure 2) over a duration of ~ 2 Myr would also indicate a full spreading rate of ~ 20 mm/yr, implying that this rate could have been nearly constant over the last 5 Myr. The central lineation with normal polarity represents the more recent Gauss epoch[38] (3.58-2.58 Ma) and records the cessation of seafloor spreading and corresponding extensional deformation in the Western Havre Trough ~2.6 Ma. The change from zone I and II, with a normal polarity central anomaly (Gauss epoch), to zone III, with a reversed polarity central anomaly (Matuyama epoch) could be an effect of the southward propagation of extension down the Havre Trough[18,21,22] with a more recent termination of seafloor spreading (~ 2.0 Ma) within zone III.

The magnetic anomaly pattern in the Eastern Havre Trough is consistent with arc magmatism, where the occurrence of bathymetry-correlated magnetic anomalies with alternating polarities reflects different ages for basins and volcanic edifices emplaced during the Matuyama and Brunhes epochs. This interpretation is partially supported by microfossil[21], K-Ar[16,21] and Ar-Ar[30,35] ages from few volcanoes of the Kermadec arc front. The Bouguer gravity map of Figure 2d supports a model of crustal thinning and a shallow upwelling of mantle material beneath Western and Eastern Havre Trough.

Figure 4 shows three cross-sectional models along the grey continuous lines a, b, and c (Figure 1) cutting zones I, II, and III, each simultaneously fitting magnetic and gravity anomalies. These models show that oceanic crust ~5 km thick, with alternating magnetic polarities in the Western Havre Trough, is needed to simultaneously reproduce geophysical observations. By contrast, the Eastern Havre Trough shows the presence of more homogenous and slightly thicker (6-7 km) crust in the active Kermadec arc front region, broadly consistent with estimates from seismic surveys[11].

Rollback and breakup of the proto-Colville-Kermadec arc

Geophysical and structural observations suggest that the opening of the Havre Trough was achieved in two distinct stages. The first stage was dominated by an initial surge of seafloor spreading which occurred soon after rifting of the proto-Colville-Kermadec arc ~ 5.5 Ma and lasted until ~3.0-2.5 Ma in zones I and II, and until ~2.0 Ma in zone III (Figure 2). The sharp termination of the magnetic lineations in the Western Havre Trough (Figure 2a) indicates an abrupt transition towards a second evolutionary stage characterized by a completely different tectono-magmatic regime. This is supported by the stark morphological contrast (Figure 3), showing evidence of arrested deformation in the Western Havre Trough and present-day rifting and arc constructional magmatism in the Eastern Havre Trough.

This model could also explain the observation that the Havre Trough and the active continental rift of the TVZ are not continuous[16,18,19,28], being sinistrally offset by ~ 50 km. Our two-stage tectonic model show that the discontinuity in the center of the Havre Trough is perfectly aligned with the western boundary of the TVZ rift (Figure 1). This suggests that the TVZ represents in fact the onshore southward continuation of the Eastern Havre Trough, where the recent stage of extension is continuously taking place since ~ 2 Ma.

The western limit of oceanic spreading defined by the boundary of the corresponding magnetic lineations, is offset ~ 15-20 km east the Colville Ridge (Figure 2). A similar distance of 15-20 km can be inferred from the seismic sections in Figure 3. This measurement approximately represents the half-width of stretched crust that could accommodate extension before seafloor spreading. A pure shear extension model applied to the Havre Trough using a stretching factor $\beta \approx 3$[32], suggests that splitting of the original proto-Colville-Kermadec arc was focussed in a very narrow, central region only ~10-13 km wide. This is also supported by the near-vertical inner margins of both the Colville and Kermadec Ridges, which are mirrored across the Havre Trough (Figure 2a and Figure 3). Even assuming a more rigid stretching factor $\beta \approx 2$ estimated for the continental TVZ[19,28] the maximum width of the break-up zone would not exceed 20 km. This zone of initial weakness constitutes only 10-15% of the original width of the proto-Colville-Kermadec arc.

General investigations of back-arc basins worldwide[2,3,9,39] have shown a significant correlation with the absolute motion of the overriding plate away from the trench and a consolidated view, supported by analogue and numerical experiments[40,41], implies that rapid rollback of the trench hinge and steepening of the subducting slab induced by the negative buoyancy of the old (and cold) subducting lithosphere[3,9] is thought to be the primary cause of extension in the overriding plate. Toroidal mantle flow around lateral slab edges, more than trench suction[3,39], is thought to induce stress and shear drag in the overriding lithosphere particularly at narrow subduction zones[42-44].

The present age of the subducting lithosphere below the Havre Trough is > 100 Ma[45], indicating that the Pacific lithosphere is old and heavy enough to sink and induce retreat of the trench. This mechanism of rollback in the Havre Trough is supported by extension directions determined from focal mechanisms[23,24], by direction of fault strikes in the TVZ rift consistent with the southeast migration of arc front volcanoes[46-48], and by the parallelism of extension direction between Colville and Kermadec Ridges[1,20,49]. Plate circuit reconstruction based on absolute velocites[9] also shows that in the Lau Basin, where mature back-arc spreading is evident[4,5,7,8], the trench has been retreating east since ~10 Ma (Figure 1), whereas in the Havre Trough trench retreat started only ~ 5 Ma, contemporaneously to our observations of back-arc spreading initiation.

Conceptual model

Three-dimensional numerical models of subduction dynamics predict that mantle flow can induce significant interaction between decompression and flux melts[42,43], with transport of depleted mantle from the back-arc to the arc[44]. Homogeneous models predict that as rollback continues, arc and back-arc melting regions become gradually disconnected over time-scales of ~ 10-15 Myr, with possible cessation of back-arc spreading for narrow subducting plates exhibiting a decrease of trench retreat velocity[44]. In the Havre Trough we observe a sharp termination of seafloor spreading, with the locus of deformation jumping from west to east after a short time-scale of ~ 3.0-2.5 Myr. The abruptness of this transition can be explained by considering the combined influence of slab rollback and local anomalies in the rheology of the mantle wedge promoted by thermal weakening, which could have induced discontinuous dynamics in the interaction between arc and back-arc melts over shorter time-scales.

Starting ~5.5 Ma (Figure 5a), trench rollback induces extension in the overriding plate with rifting involving a narrow region of the active proto-Colville-Kermadec arc where the crust is weakest, immediately followed by seafloor spreading. As the Pacific Plate rolls back (Figure 5b), the path taken by ascending arc melts towards the surface is deflected westward by pre-existing permeable zones of thermal weakness in the mantle wedge, underlying the region of seafloor spreading. This deflection cannot continue indefinitely, because at some point the ongoing rollback of the Pacific Plate will induce the trajectory of arc melts to snap back realigning surface volcanism with the source of arc melts at depth, ultimately diverting the arc flux outside of the region of seafloor spreading (Figure 5c). As the back-arc region in the Western Havre Trough cools down, it becomes essentially an inactive microplate locked to the overriding Australian Plate, and the active Kermadec arc front in the Eastern Havre Trough is the new locus of active extension.

If this model constitutes the general mechanism for the early opening of back-arc basins, it could explain similar observations of extinct, short-term episodic back-arc spreading centres that are observed in other subduction systems, such as the Tyrrhenian Sea[50,51] and the Okinawa Trough[52]. In agreement with recent studies of continental rifting[53,54], a fast surge of seafloor spreading was the first mechanism of crustal accretion in the Havre Trough and occurred shortly after the breakup of a very narrow region of the original proto-Colville-Kermadec arc.

References

1. Karig, D.E. Ridges and basins of the Tonga-Kermadec island arc system. *J. Geoph. Res.* **75**, 239-254, doi: 10.1029/JB075i002p00239 (1970).
2. Packham, G.H. & Falvey, D.A. An hypothesis for the formation of marginal seas in the western Pacific. *Tectonophysics* **11**, 79-109, doi: 10.1016/0040-1951(71)90058-8 (1971).
3. Molnar, P. & Atwater, T. Interarc spreading and Cordilleran tectonics as alternates related to the age of subducted oceanic lithosphere. *Earth Planet. Sci. Lett.* **41**, 330-340, doi: 10.1016/0012-821X(78)90187-5 (1978).
4. Martinez, F. & Taylor, B. Modes of crustal accretion in backarc basins: inferences from the Lau Basin. In: Christie, D.M., Fisher, C.R., Lee, S.-M., Givens, S. (Eds.), Backarc Spreading Systems: Geological, Biological, Chemical and Physical Interactions. *Geoph. Mon. Ser.* **166**. American Geophysical Union, 5–30, doi: 10.1029/166GM03 (2006).
5. Dunn, R. & Martinez, F. Contrasting crustal production and rapid mantle transitions beneath back-arc ridges. *Nature* **469**, 198-202, doi: 10.1038/nature09690 (2011).
6. Martinez, F., Fryer, P., Baker, N.A. & Yamazaki, T. Evolution of backarc rifting: Mariana Trough, 20°-24° N. *J. Geoph. Res.* **100**, 3807-3827, doi: 10.1029/94JB02466 (1995).
7. Martinez, F. & Taylor, B. Mantle wedge control on back-arc crustal accretion. *Nature* **416**, 417-421, doi: 10.1038/416417a (2011).
8. Taylor, B., Zellmer, K., Martinez, F. & Goodliffe, A. Sea-floor spreading in the Lau back-arc basin. *Earth Planet. Sci. Lett.* **144**, 35-40, doi: 10.1016/0012-821X(96)00148-3 (1996).
9. Sdrolias, M. & Müller, R.D. Controls on back-arc formation. *Geochem. Geophys. Geosyst.* **7**, Q04016, doi: 10.110.1029/2005GC001090 (2006).

10. O’ Neill, C.J., Müller, R.D. & Steinberger, B. On the uncertainties in hotspot reconstructions and the significance of moving hotspot reference frames. *Geochem. Geophys. Geosyst.* **6**, Q04003, doi:10.1029/2004GC000784 (2005).

11. Bassett, D. *et al.* Crustal structure of the Kermadec arc from MANGO seismic refraction profiles. *J. Geoph. Res.* **121**, 7514-7546, doi: 10.1002/2016JB013194 (2016).

12. Timm, C., *et al.* Subduction of the oceanic Hikurangi Plateau and its impact on the Kermadec arc. *Nat. Commun.* **5**, 4923, doi: 10.1038/ncomms5923 (2014).

13. Fujiwara, T., Yamazaki, T. & Joshima, M. Bathymetry and magnetic anomalies in the Havre Trough and southern Lau Basin: from rifting to spreading in back-arc basins. *Earth Planet. Sci. Lett.* **185**, 253-264, doi: 10.1016/S0012-821X(00)00378-2 (2001).

14. Delteil, J., Ruellan, E., Wright, I. & Matsumoto, T. Structure and structural development of the Havre Trough (SW Pacific). *J. Geoph. Res.* **107**, 21043-2106, doi: 10.1029/2001JB000494 (2002).

15. Caress, D. Structural trends and back-arc extension in the Havre Trough. *Geoph. Res. Lett.* **18**, 853-856, doi: 10.1029/91GL01060 (1991).

16. Wright, I. Pre-spread rifting and heterogeneous volcanism in the Southern Havre Trough back-arc basin. *Mar. Geol.* **113**, 179-200, doi: 10.1016/0025-3227(93)90017-P (1993).

17. Wright, I. Nature and tectonic setting of the southern Kermadec submarine arc volcanoes: An overview. *Mar. Geol.* **118**, 217-236, doi: 10.1016/0025-3227(94)90085-X (1994).

18. Parson, L. & Wright I. The Lau-Havre-Taupo back-arc-basin: A southward-propagating, multi-stage evolution from rifting to spreading. *Tectonophys.* **263**, 1-22, doi: 10.1016/S0040-1951(96)00029-7 (1996).

19. Stern, T.A. Asymmetric back-arc spreading, heat flux and structure associated with the Central Volcanic Region of New Zealand. *Earth Planet. Sci. Lett.* **85**, 265-276, doi: 10.1016/0012-821X(87)90037-9 (1987).

20. Wright, I., Parson, L. & Gamble, J. Evolution and interaction of migrating cross-arc volcanism and back-arc rifting: An example from the Southern Havre Trough (35°20' - 37° S). *J. Geoph. Res.* **101**, 22071-22086, doi: 10.1029/96JB01761 (1996).

21. Ballance *et al.* Morphology and history of the Kermadec trench-arc-backarc basin-remnant arc system at 30 to 32° S: geophysical profile, microfossil and K-Ar data. *Mar. Geol.* **159**, 35-62, doi: 10.1016/S0025-3227(98)00206-0 (1993).

22. Ruellan, E., Delteil, J., Wright, I. & Matsumoto, T. From rifting to active spreading in the Lau Basin – Havre Trough backarc system (SW Pacific): Locking/unlocking induced by seamount chain subduction. *Geochem. Geophys. Geosyst.* **4**, 8909-8930, doi: 10.1029/2001GC000261 (2003).

23. Seebeck, H., Nicol, A., Giba, M., Pettinga, J. & Walsh, J. Geometry of the subducting Pacific plate since 20 Ma, Hikurangi margin, New Zealand. *J. Geol. Soc. Lon*. **171**, 131-143, doi: 10.1144/jgs2012-145 (2014).

24. Seebeck, H., Nicol, A., Villamor, P., Ristau, J. & Pettinga, J. Structure and kinematics of the Taupo Rift, New Zealand, *Tectonics* **33**, 1178-1199, doi: 10.1002/2014TC003569 (2014).

25. Walcott, R.I. The kinematics of the plate boundary zone through New Zealand: a comparison of short and long-term deformation, *Geoph. J., R. Astron. Soc*. **79**, 613-633, doi: 10.1111/j.1365-246X.1984.tb02244.x (1984).

26. Darby, D.J. & Williams, R.O. A new geodetic estimate of deformation in the Central Volcanic Region of the North Island, New Zealand, *N. Zeal. J. Geol. Geoph.* **34**, 127-136, doi: 10.1080/00288306.1991.9514450 (1991).

27. Pelletier, B. & Loutat, R. Seismotectonics and present-day relative plate motions in the Tonga-Lau and Kermadec-Havre region, *Tectonophysics* **165**, 237-250, doi: 10.1016/0040-1951(89)90049-8 (1989).

28. Davey, F.J., Henrys, S. & Lodolo, E. Asymmetric rifting in a continental back-arc environment, North Island, New Zealand, *J. Volcanol. Geoth. Res.* **68**, 209-238, doi: 10.1016/0377-0273(95)00014-L (1995).

29. Wallace, L.M. Ellis, S. & Mann, P. Collisional model for rapid fore-arc block rotations, arc curvature, and episodic back-arc rifting in subduction settings, *Geochem. Geophys. Geosyst.* **10**, Q05001, doi: 10.110.1029/2005GC002220 (2009).

30. Timm, C., *et al*. New Age and Geochemical Data from the Southern Colville and Kermadec Ridges, SW Pacific: Insights into the recent geological history and petrogenesis of the Proto-Kermadec (Vitiaz) Arc. *Gondwana Res.* **72**, 169-193, doi: 10.1016/j.gr.2019.02.008 (2019).

31. Malahoff, A., Feden, R. & Fleming, H. Magnetic anomalies and tectonic fabric of marginal basins north of New Zealand. *J. Geoph. Res.* **87**, 4109-4125, doi: 10.1029/JB087iB05p04109 (1982).

32. Wysoczanski, R.J., *et al.* Backarc rifting, constructional volcanism and nascent disorganized spreading in the southern Havre Trough backarc rifts (SW Pacific). *J. Volcanol. Geoth. Res.* **190**, 39-57, doi: 10.1016/j.jvolgeores.2009.04.004 (2010).

33. Sandwell, D. T. & Smith, W. H. F. Marine gravity anomalies from Geosat and ERS 1 satellite altimetry. *J. Geoph. Res.* **102**, 10039-10054, doi: 10.1029/96JB03223 (1997).

34. Todd E., *et al.* Sources of constructional cross-chain volcanism in the southern Havre Trough: New insights from HFSE and REE concentration and isotope systematics. *Geochem. Geophys. Geosyst.* **7**, Q04009, doi:10.1029/2009GC002888 (2011).

35. Wysoczanski, R.J., *et al.* Ar-Ar age constraints on the timing of Havre Trough opening and magmatism. *N. Zeal. J. Geol. Geoph.*, doi.org/10.1080/00288306.2019.1602059 (2019).

36. Pillans, B. & Wright, I. Late Quaternary tephrostratigraphy for the Southern Havre Trough – Bay of Plenty, northeast New Zealand. *N. Zeal. J. Geol. Geoph.* **35**, 129-143, doi: 10.1080/00288306.1992.9514507 (1992).

37. Cronan, D.S., Hodkinson, R., Harkness, D.D., Moorby, S.A. & Glasby, G.P. Accumulation rates of hydrothermal metalliferous sediments in the Lau Basin, S.W. Pacific. *Geo-Mar. Lett.* **6**, 51-56, doi: 10.1007/BF02311696 (1986).

38. Cande, S. & Kent, D. Revised calibration of the geomagnetic polarity timescale for the Late Cretaceous and Cenozoic. *J. Geoph. Res.* **100**, 6093-6095, doi: 10.1029/94JB03098 (1995).

39. Heuret, A. & Lallemand, S. Plate motions, slab dynamics and back-arc deformation. *Phys. Earth Planet. Inter.* **149**, 31-51, doi: 10.1016/j.pepi.2004.08.022 (2005).

40. Faccenna, C., Funiciello, D., Giardini, D. & Lucente, P. Episodic back-arc extension during restricted mantle convection in the Central Mediterranean. *Earth Planet. Sci. Lett.* **187**, 105-116, doi: 10.1016/S0012-821X(01)00280-1 (2001).

41. Schellart, W.P.G., Lister, G.S., & Jessell, M.N. Analogue modelling of arc and backarc deformation in the New Hebrides Arc and North Fiji Basin, *Geology* **30**, 311-314, doi: 10.1130/0091-7613 (2002).

42. Billen, M.I. Modeling the dynamics of subducting slabs, *Ann. Rev. Earth Planet. Sci.* **36**, 325-356, doi: 10.1146/annurev.earth.36.031207.124129 (2008).

43. Schellart, W.P. & Moresi, L. A new driving mechanism for backarc extension and backarc shortening through slab sinking induced toroidal and poloidal mantle flow: Results

from dynamic subduction models with an overriding plate. *J. Geoph. Res.* **118**, 3221-3248, doi: 10.1002/jgrb.50173 (2013).

44. Magni, V. The effects of back-arc spreading on arc magmatism. *Earth Planet. Sci. Lett*. **519**, 141-151, doi: 10.1016/j.epsl.2019.05.009 (2019).

45. Müller, R.D., Sdrolias, M., Gaina, C. & Roest, W.R. Age, spreading rates, and spreading asymmetry of the world's ocean crust. *Geochm. Geophys. Geosyst*. **9**, 1-19, doi: 10.1029/2007GC001743 (2008).

46. Brothers, R.N. Subduction regression and oceanward migration of volcanism, North Island, New Zealand, *Nature* **309**, 698-700, doi: 10.1038/309698a0 (1984).

47. Kamp, P.J.J. Neogene and Quaternary extent and geometry of the subducted Pacific Plate beneath North Island, New Zealand: Implications for Kaikoura tectonics, *Tectonophysics* **108**, 241-246, doi: 10.1016/0040-1951(84)90238-5 (1984).

48. Mortimer, N., Gans P.B., Palin, J.M., Meffe, S., Herzer, R.H. & Skinner, D.N.B. Location and migration of Miocene-Quaternary volcanic arcs in the SW Pacific region, *J. Volcanol. Geotherm. Res.* **190**, 1-10, doi: 10.1016/j.jvolgeores.2009.02.017 (2010).

49. Wright, I.C. Morphology and evolution of the remnant Colville and active Kermadec arc ridges south of 33 30' S, *Mar. Geoph. Res.* **19**, 177-193, doi: 10.1023/A:10042669 (1997).

50. Malinverno, A. & Ryan, W.B.F. Extension in the Tyrrhenian Sea and shortening in the Apennines as result of arc migration driven by sinking of the lithosphere. *Tectonics* **5**, 227-245, doi: 10.1029/TC005i002p00227 (1986).

51. Nicolosi, I., Speranza, F. & Chiappini, M. Ultrafast oceanic spreading of the Marsili Basin, southern Tyrrhenian Sea: Evidence from magnetic anomaly analysis. *Geology* **34**, 717-720, doi: 10.1130/G22555.1 (2006).

52. Sibuet, J.C. *et al.* Back arc extension in the Okinawa Trough. *J. Geoph. Res.* **92**, 14041-14063, doi: 10.1029/JB092iB13p14041 (1987).

53. Brune, S., Williams, S.E., Butterworth, N.P. & Müller, D. Abrupt plate accelerations shape rifted continental margins. *Nature* **536**, 201-204, doi: 10.1038/nature18319 (2016).

54. Larsen, H.C. *et al.* Rapid transition from continental breakup to igneous oceanic crust in the South China Sea. *Nat. Geosci*. **11**, 782–789, doi: 10.1038/s41561-018-0198-1 (2018).

Corresponding author

Correspondence about the manuscript and requests for material should be addressed to:

Fabio Caratori Tontini

GNS Science

PO Box 30368, Lower Hutt 5040, New Zealand

Email: f.caratori.tontini@gns.cri.nz

Acknowledgements

We acknowledge the Captains and Crews of R/V Yokosuka, Sonne, Tangaroa, Roger Revelle and Thompson for their hard work to support geophysical and bathymetry data acquisition. Funding from New Zealand government helped enable this study and assist scientists with cruise travels and survey operations.

Author contributions

F.C.T., C.D.R. and C.T. conceived the project and developed the conceptual model; D.B. contributed to seismic interpretation and to the conceptual model; R.W. contributed to the tectonic and volcanology interpretation. All authors contributed to writing the manuscript.

Financial and non-financial competing interests

None

Figure captions

Figure 1: **Location map of the Havre Trough and subduction of the Pacific Plate underneath the Australian Plate**. Absolute plate velocities relative to a reference frame tied to the moving Atlantic-Indian ocean hot-spots[9,10]. The white lines represent the reconstructed position of the trench since 10 Ma[9] (triangle line showing present day trench position). Grey solid line M4 is the MANGO[11] seismic reflection/refraction profile shown in Figure 3. Grey solid lines a, b, and c are the interpreted profiles (a), (b) and (c) in Figure 4. The grey dashed line is the approximate location of the median line separating Western from Eastern Havre Trough. Black dashed line encloses present-day continental rift of the Taupo Volcanic Zone (TVZ).

Figure 2: **Bathymetric and geophysical maps of the Havre Trough.** a) Bathymetry map. Inset shows the survey area in relation to New Zealand landmass; b) Total-intensity magnetic anomaly map, reduced-to-the-pole; c) Gravity anomaly, free-air from shipborne data and complemented with satellite gravity[33]; d) Bouguer gravity anomaly subtracting the effects of bathymetry. The two black dashed lines enclose the Western Havre Trough, with orthogonal short black lines delimiting the boundaries of zones I, II, and III.

Figure 3: **Multichannel seismic section M4 from Mango experiment[11].** a) OBS velocity model. Inset shows the seismic reflection data displayed in (b); b) seismic reflection data. A buried ridge is visible as an increase of P-wave velocity at ~ 82 km horizontal distance in (a), corresponding to thinner sediments and shallower basement in the seismic reflection data in (b) around CPD 570.

Figure 4: **Geophysical models of the Havre Trough along the three continuous lines in Figure 1.** a) Zone I; b) Zone II; c) Zone III; d) Legend with colours, symbols, density and magnetization parameters. δ and M indicate density and magnetization, respectively. CR is

Colville Ridge, KR is Kermadec Ridge. The progressive change in the central anomaly from Gauss to Matuyama[38] from (a) to (c) indicates the more recent seafloor spreading in the Western Havre Trough consistent with progressive southward migration of extensional deformation[18,21,22]. Crustal thinning up to 4-5 km is evident under the Western Havre Trough.

Figure 5: **Conceptual model of the Havre Trough opening, section view (left) and map sketch (right**). a) Initial arc flux induced by subduction of the Pacific Plate with rate V_S, overriding plate advancing with velocity V_O; b) Extension with rate V_E induced by trench retreat with velocity V_T, seafloor spreading and westward deflection of the arc flux; c) Jump in the trajectory of arc melts, realigning surface volcanism with arc magma genesis at depth, trajectory of arc melts ~ 2.5 Ma shown in light blue. PCKA is the proto-Colville-Kermadec arc, KAF is the Kermadec arc front, CR is the Colville Ridge, KR is the Kermadec Ridge, FM is flux melting, DM is decompression melting.

Methods

Magnetic and gravity data: acquisition and processing.

Gravity and magnetic data were processed using Geosoft Oasis Montaj® software. Magnetic data were collected during twelve cruises (see Supplementary Table 1) from 2004 to 2018, supplemented by low-altitude aeromagnetic data[31] and shipborne data from NGDC database (https://www.ngdc.noaa.gov/mgg/geodas/trackline.html). Shipborne magnetic data were processed for heading and lag errors. Magnetic anomalies were obtained removing the International Geomagnetic Reference Field[55] (IGRF). The total-intensity magnetic anomalies were reduced-to-the-magnetic pole[56] to remove any skewness effect coming from the dipole shape of the magnetic field at mid-latitudes.

Shipborne gravity data were collected during nine cruises (see Supplementary Table 1) also from 2004 to 2018. These data were supplemented by satellite altimetry-derived gravity data[33]. Shipborne gravity data were corrected for drift and Eotvos effects and processed with a 120 s long Butterworth low-pass filter along the survey lines. The shipborne gravity data cross-over error with the satellite-derived gravity data was within 2 mGal. The Bouguer gravity anomaly, which removes the effect of the seafloor topography from the free-air anomaly, was calculated using a standard reduction density of 2.67 g cm^{-3}.

Both gravity and magnetic data were smoothed using a low-pass desampling filter and gridded with a common cell-size of 500 m using a minimum-curvature algorithm[57,58] to interpolate the irregularly-spaced line-data and fill gaps between the survey lines using a Maximum Entropy Prediction algorithm[59]. The geophysical models in Figure 4 were produced extracting data along the selected profiles from the co-located bathymetry, gravity and magnetic grids. These profiles were modelled using 2-D polygonal bodies[60] with infinite length along the strike perpendicular to the profiles.

Seismic data: acquisition and processing.

Seismic reflection data were acquired onboard RV Sonne voyage SO192-1 as part of the Marine Geoscientific Investigations on the Input and Output of the Kermadec Subduction Zone – MANGO[11,61]. The seismic source comprised two G-gun clusters with a combined volume of 64 litres at 3000 psi. Seismic data was recorded by a 16-channel streamer from GNS Science, with 2m hydrophone spacing. Towing depth was 8 m and the 60 sec shot intervals at 5 knots was optimized for the acquisition of Ocean Bottom Seismometer data.

These multichannel seismic data were processed at GNS Science using GLOBE Claritas® software. After sorting and stacking across common shot-points, we applied a simple processing sequence involving resampling at 4 ms, band-pass frequency filtering (corner frequencies 1-20-120-180 Hz), Automatic-Gain Control (AGC) over 14 s window, surgical muting of the direct arrival. The resulting stack was trimmed to 14 second record length and output as SEG-Y.

Magnetic chronology and opening of the Havre Trough.

The magnetic anomalies in the Western Havre Trough show a pattern of lineations corresponding to different polarities. The Plio-Pleistocene is characterized by four magnetic epochs with alternating reversed and normal polarities (see Supplementary Table 2). Within each of these epochs, short reversal chrons (~ 0.1 Ma duration) occurred, although these events are undetectable given the resolution of our magnetic compilation. Some asymmetry can be seen in the shape and width of the magnetic anomalies as is commonly observed in other back-arc basins[1,2,19,62].

Based on external constraints on ages[13,16,18,20-22] of the initial opening of the Havre Trough and extension rates[16,18,20], the optimal combination of magnetic epochs which could explain the observed magnetic lineations in zones I and II (Figure 2) is Gilbert (reversed) and Gauss (normal), between 5.89 Ma and 2.58 Ma, respectively. For our calculations we then adopted a full spreading rate R=20 mm/yr, estimated as an average value from present-day observations[25-29], and we use the average width w of the magnetic anomaly to independently date the opening of the Havre Trough and check consistency with other studies of ages and rates:

$$\Delta T = R\, w\,, \tag{1}$$

where ΔT is the duration of seafloor spreading recorded by the magnetic anomaly during a specific epoch.

In zone I (Fig. 2), the average total-width of the negative lineations corresponding to the Gilbert epoch is ~ 35-40 km wide (see Supplementary Figure 1), which implies a duration ΔT ~ 1.8-2.0 Myr. This anomaly records the inception of seafloor spreading which then started 1.8-2.0 Myr before the beginning of the Gauss epoch (or end of the Gilbert epoch), i.e., 5.3-5.6 Ma. The average width of the lineation corresponding to the Gauss epoch is ~20 km, which gives ΔT ~ 1.0 Myr. This is the central anomaly which recorded the cessation of seafloor spreading which therefore terminated ~1.0 Myr after the beginning of the Gauss epoch, i.e., 2.6 Ma. This age is close to the beginning of the Matuyama reversed epoch, which could explain the presence of small negative anomalies right on the center of the Gauss central anomaly, as they could have recorded the last and more recent episodes of seafloor spreading at the beginning of the Matuyama epoch with reversed polarity. In zone II (Figure 2) we have similar widths of ~ 35-40 km for the Gilbert and 20 km for the Gauss central anomaly, respectively.

This suggests similar ages for seafloor spreading in this zone, although here the magnetic lineations are more curved and less linear than in zone I. If this is not an artefact from interpolation, it could suggest that concomitant action of other mechanisms of tectonic deformation may have played a role in shaping up these anomalies in the transition zone between zone I and III (Figure 2). In zone III, the central anomaly is reversed, with an average width of ~ 12 km. Our interpretation of this anomaly is that it has recorded the last episode of seafloor spreading in zone III, and it was emplaced during the early Matuyama epoch, which is consistent with the progressive southward propagation of extension in the Havre Trough[18,21,22]. The width of 12 km corresponds to a duration of ~0.6 Myr, which gives an age of ~2.0 Myr for the termination of seafloor spreading in this area.

Another possible pattern of reversed and normal polarities occurred during the Matuyama and Brunhes epochs, respectively, between 2.58 Ma and present day, but these magnetic epochs cannot explain the magnetic lineations because they would imply unrealistic kinematic models. For example, the sediments thickness in the Western Havre Trough implies absence of consistent deformation in this area for a significant amount of time. Even assuming a sudden jump of the full spreading rate up to ~100 mm/yr towards the end of the seafloor spreading phase in the Western Havre Trough, it would require at least ~ 0.2 Ma to reproduce the observed width of ~ 20 km of the central lineation of normal polarity in Zones I and II. If this happened during the normal polarity Brunhes epoch, then seafloor spreading terminated ~ 0.58 Ma, (i.e., 0.2 Myr after the beginning of the Brunhes epoch, see Supplementary Table II). In this case, ~180 m of sediments in the Western Havre Trough (Figure 3) had to be deposited in 0.58 Myr. This in turn would give an unrealistic sedimentation rate > 300 mm/kyr.

More importantly, the width of the Eastern Havre Trough is representative of the most recent phase of extensional deformation which occurred after the cessation of back-arc oceanic spreading in the Western Havre Trough. Even assuming a sudden inception of extensional deformation in the Eastern Havre Trough starting ~ 0.58 Ma, a full rate of ~ 100 mm/yr would also be needed to reproduce the observed width of the Eastern Havre Trough (~50-60 km), which strongly disagrees with the present-day observed rate of ~20 mm/yr. In summary, the interpretation of the magnetic lineations using Matuyama and Brunhes epochs would require unrealistic, discontinuous kinematic models characterized by slow extension rate during the first phase of opening of the Havre Trough followed by an abrupt increase in spreading rates to more than 100 mm/yr occurring during the Brunhes epoch.

Pure shear extension model.

We used a pure shear[63] model for extension, where a certain region of the lithosphere extends and thins under tensional stresses, maintaining a constant volume. This model is controlled by the stretching factor β, which defines the amount of horizontal stretching or vertical thinning of the deformed region (see Supplementary Figure 2). This model is obviously an oversimplification of the real process of extension, but could be used to roughly estimate some parameters such as the original width L where initial rifting and deformation of the old arc occurred, by introducing estimates of the stretching factor β. These values of β are poorly constrained, but typical values are in the range 1-2 for intracontinental basins, gradually increasing to 2-4 for offshore oceanic crust[64]. In the specific case of the continental rift in New Zealand, a value of β=2 was estimated from geophysical models in the TVZ[19,28]. A value of β=3 was proposed as a better estimate in the Havre Trough[32]. This value is in agreement with the crustal models in Figure 4, which show an average thickness of the pre-spreading old thinned and rifted arc crust ~ 3 km (L/β), and an average thickness of the Colville and Kermadec Ridges of 10 km (L), which in turn imply a value of β~3.3.

Data availability

The survey magnetic data can be downloaded from the NGDC database https://ngdc.noaa.gov/mgg/geodas/trackline.html. The gravity data derived from satellite altimetry can be downloaded from https://topex.ucsd.edu/marine_grav/mar_grav.html. The regional bathymetry grid shown in Figure 1 can be downloaded from https://www.niwa.co.nz/our-science/oceans/bathymetry. The high-resolution bathymetry and geophysical grids used in this study are available from the corresponding author upon request.

References (only in methods)

55. Thebault, E. *et al.* International Geomagnetic Reference Field: the 12th generation. *Earth Planet. Sp.*, 67-79, doi:10.1186/s40623-015-1228-9 (2015).

56. Baranov, V. & Naudy, H. Numerical calculation of the formula of reduction to the magnetic pole. *Geophys.* **29**, 67-79, doi: 10.1190/1.1439334 (1964).

57. Briggs, I.C. Machine contouring using minimum curvature. *Geophysics* **39**, 39-48, doi: 10.1190/1.1440410 (1964).

58. Smith, W.H.F. & Wessel, P. Gridding with continuous curvature splines in tension. *Geophys.* **55**, 293-305, doi: 10.1190/1.1442837 (1990).

59. Ulrych, T.J. Maximum entropy power spectrum of truncated sinusoids. *J. Geoph. Res.* 77, 1396-1400, doi: 10.1029/JB077i008p01396 (1972).

60. Won, I.J. & Bevis, M. Computing the gravitational and magnetic anomalies due to polygon: Algorithm and Fortran subroutines. *Geophys.* **52**, 232-238, doi: 10.1190/1.1442298 (1987).

61. Scherwath, M., *et al.* Fore-arc deformation and underplating at the northern Hikurangi margin, New Zealand. *J. Geoph. Res.* 115, B06408, doi: 10.1029/2009JB006645 (2010).

62. Barker, P.F. & Hill, I.A. Asymmetric spreading in back-arc basins. *Nature* **285**, 652-654, doi: 10.1038/285652a0 (1980).

63. McKenzie, D. Some remarks on the development of sedimentary basins. *Earth Planet. Sci. Lett.* **40**, 25-32, doi: 10.1016/0012-821X(78)90071-7 (1978).

64. Beardsmore G.R. & Cull J.P. Crustal heat flow. Cambridge University Press, Cambridge, United Kingdom, doi: 10.1017/CBO9780511606021 (2001).

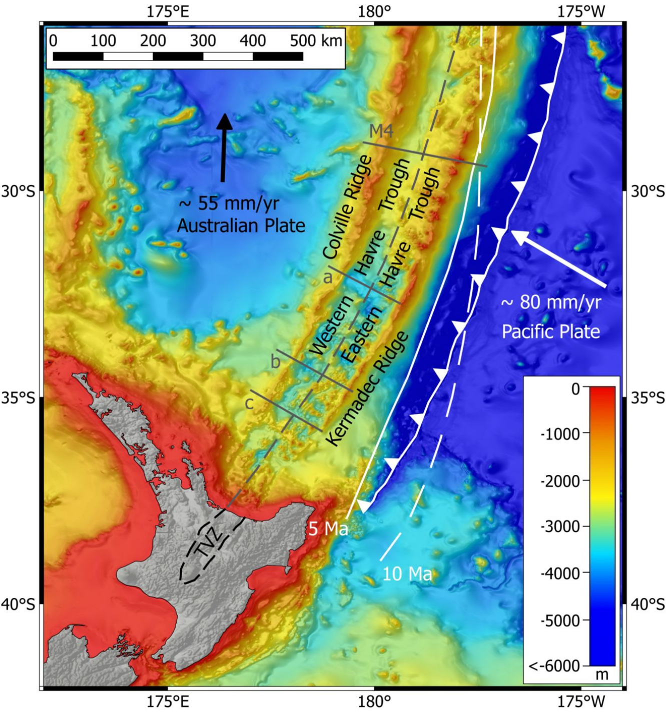

175°E
180°
175°W
0 100 200 300 400 500 km
M4
30°S
~ 55 mm/yr
Australian Plate
Colville Ridge
Trough
Trough
Havre
Havre
a
Western
Eastern
Kermadec Ridge
b
c
~ 80 mm/yr
Pacific Plate
35°S
TVZ
5 Ma
10 Ma
40°S
0
-1000
-2000
-3000
-4000
-5000
<-6000
m

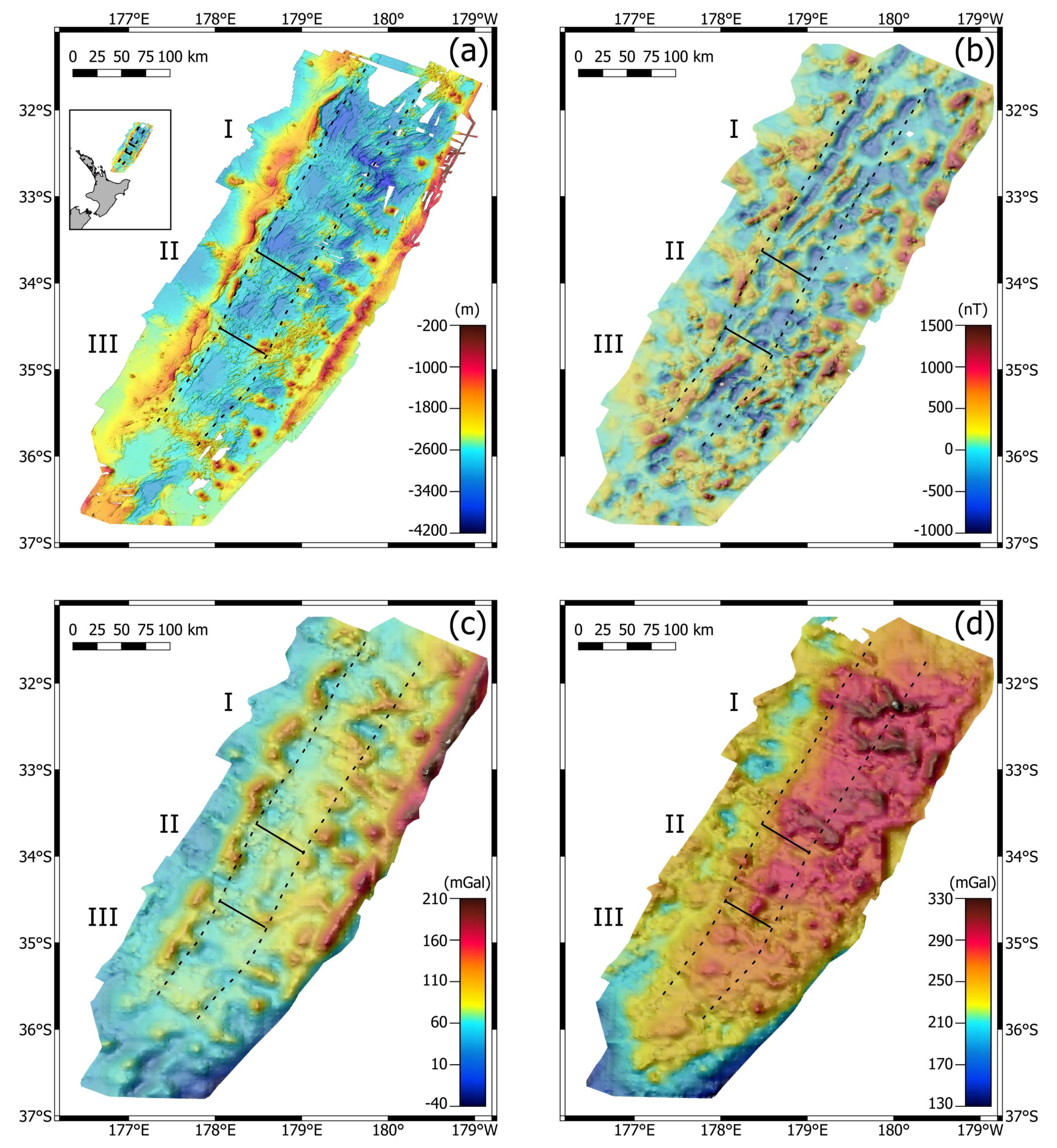

(a)
(b)
(c)
(d)
0 25 50 75 100 km
I
II
III
177°E
178°E
179°E
180°
179°W
32°S
33°S
34°S
35°S
36°S
37°S
(m)
-200
-1000
-1800
-2600
-3400
-4200
(nT)
1500
1000
500
0
-500
-1000
(mGal)
210
160
110
60
10
-40
(mGal)
330
290
250
210
170
130

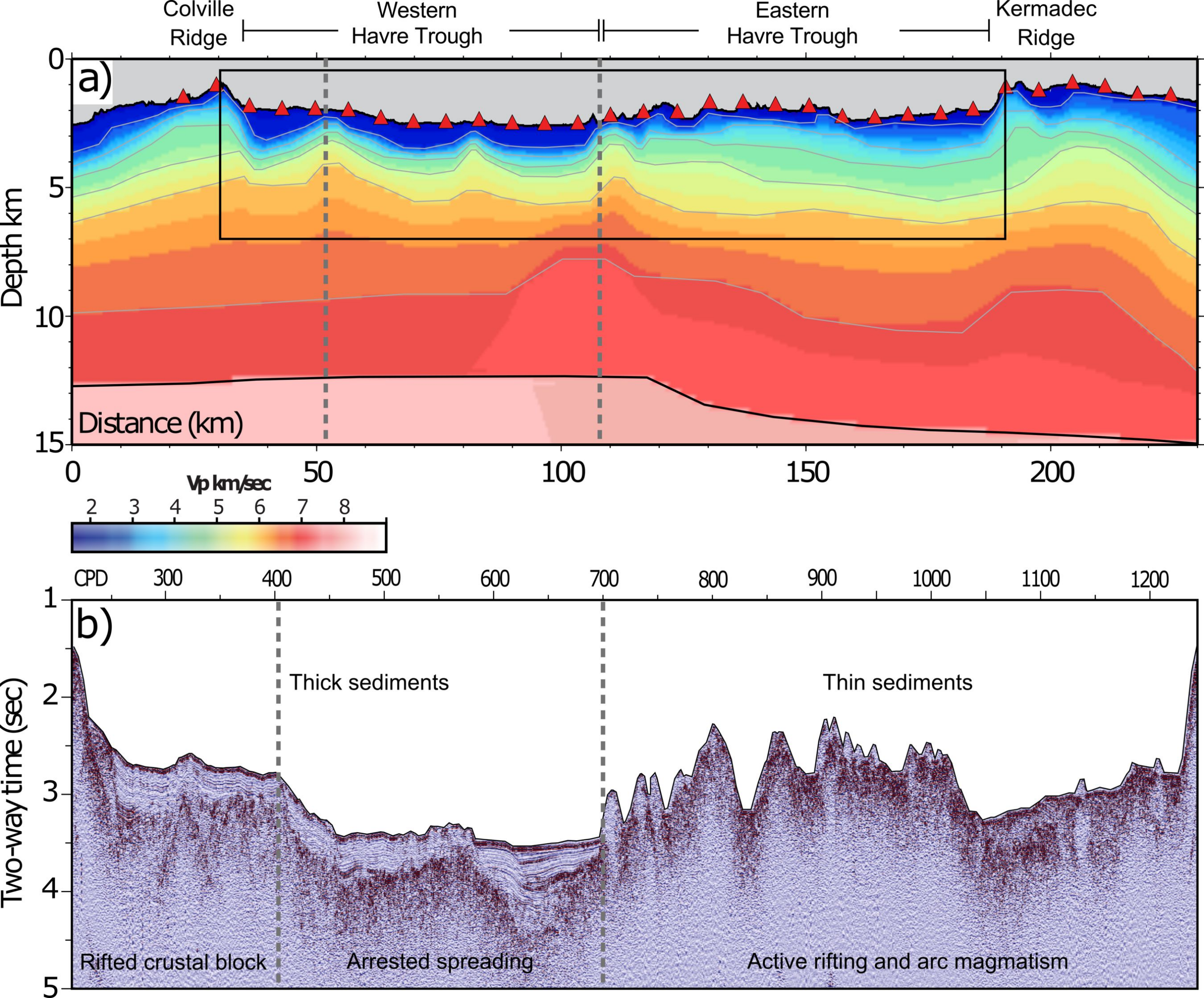

Colville Ridge
Western Havre Trough
Eastern Havre Trough
Kermadec Ridge
a)
Depth km
0
5
10
15
Distance (km)
0
50
100
150
200
Vp km/sec
2
3
4
5
6
7
8
CPD
300
400
500
600
700
800
900
1000
1100
1200
b)
Two-way time (sec)
1
2
3
4
5
Thick sediments
Thin sediments
Rifted crustal block
Arrested spreading
Active rifting and arc magmatism

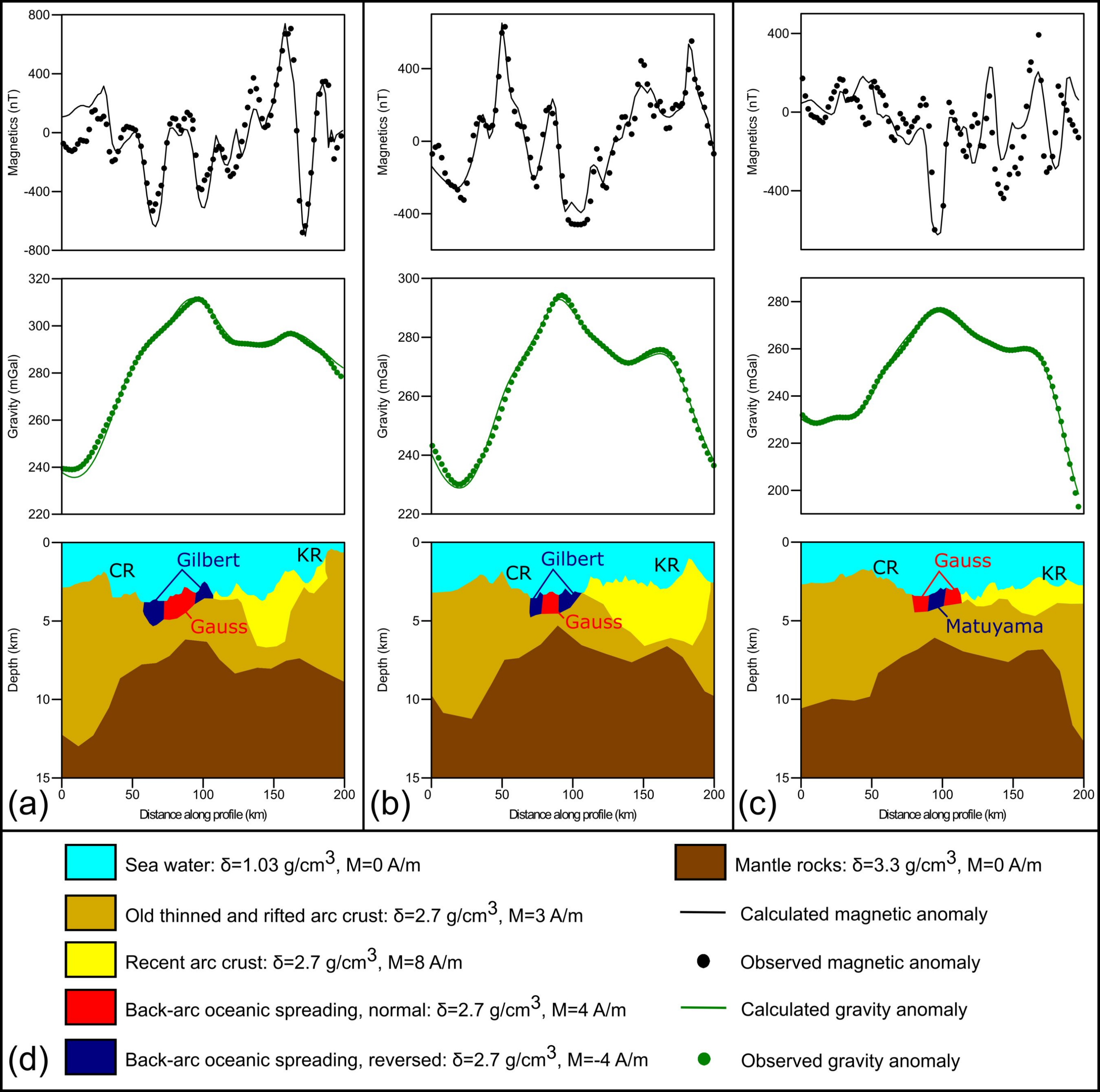

Magnetics (nT)
Gravity (mGal)
Depth (km)
CR
Gilbert
Gauss
KR
Matuyama
Distance along profile (km)
(a)
(b)
(c)
(d)
Sea water: δ=1.03 g/cm3, M=0 A/m
Old thinned and rifted arc crust: δ=2.7 g/cm3, M=3 A/m
Recent arc crust: δ=2.7 g/cm3, M=8 A/m
Back-arc oceanic spreading, normal: δ=2.7 g/cm3, M=4 A/m
Back-arc oceanic spreading, reversed: δ=2.7 g/cm3, M=-4 A/m
Mantle rocks: δ=3.3 g/cm3, M=0 A/m
Calculated magnetic anomaly
Observed magnetic anomaly
Calculated gravity anomaly
Observed gravity anomaly

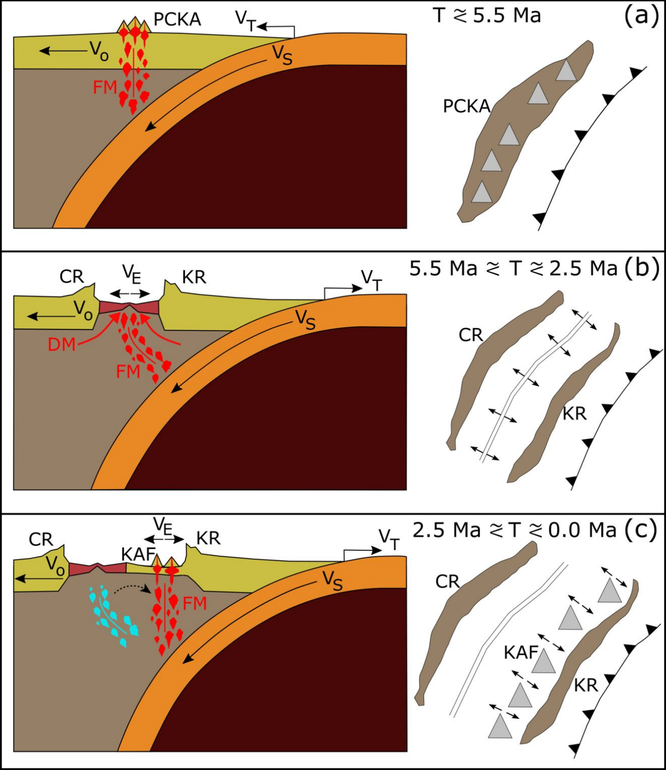

T ≈ 5.5 Ma
(a)
PCKA
V_T
V_o
V_S
FM
PCKA
5.5 Ma ≈ T ≈ 2.5 Ma
(b)
CR
V_E
KR
V_T
V_o
V_S
DM
FM
CR
KR
2.5 Ma ≈ T ≈ 0.0 Ma
(c)
CR
V_E
KR
KAF
V_T
V_o
V_S
FM
CR
KAF
KR